Proceedings of the ASME 2013 International Design Engineering Technical Conferences and Computers and Information in Engineering Conference
IDETC/CIE 2013
August 4-7, 2013, Portland, Oregon, USA

DETC2013-13037

OPTIMAL DESIGN OF THE IRSBOT-2 BASED ON AN OPTIMIZED TEST TRAJECTORY

Coralie Germain[◇], **Stéphane Caro**[∇], **Sébastien Briot**[∇], **Philippe Wenger**[∇]
[◇] LUNAM Université, Ecole Centrale Nantes, Institut de Recherche en Communications et Cybernétique de Nantes
[∇] CNRS, Institut de Recherche en Communications et Cybernétique de Nantes, UMR CNRS n° 6597
1 rue de la Noë, 44321 Nantes, France
Email: {germain, caro, briot, wenger}@irccyn.ec-nantes.fr,

ABSTRACT

This paper deals with the design optimization of the IRSBot-2 based on an optimized test trajectory for fast pick and place operations. The IRSBot-2 is a two degree-of-freedom translational parallel manipulator dedicated to fast and accurate pick-and-place operations.

First, an optimization problem is formulated to determine the optimal test trajectory. This problem aims at finding the path defined with s-curves and the time trajectory that minimize the cycle time while the maximum acceleration of the moving platform remains lower than 20 G and the time trajectory functions are C_2 continuous.

Then, two design optimization problems are formulated to find the optimal design parameters of the IRSBot-2 based on the previous optimal test trajectory. These two problems are formulated so that they can be solved in cascade. The first problem aims to define the design parameters that affect the geometric and kinematic performances of the manipulator. The second problem is about the determination of the remaining parameters by considering elastostatic and dynamic performances.

Finally, the optimal design parameters are given and will be used for the realization of an industrial prototype of the IRSBot-2.

1 INTRODUCTION

Nowadays parallel robots are used more and more in high-speed pick-and-place operations. The drive for higher operational speeds and higher payload-to-weight ratios is shifting their designs to more lightweight architectures [1, 2]. The fastest industrial robot, the Quattro by Adept Technologies Inc. [3], reaches more than 15 G of acceleration, allowing up to four standard pick-and-place cycles to be performed per second. However, as for all high-speed mechanisms, vibratory phenomena appear that worsen accuracy and dynamic performance. This crucial issue prevents from using high-speed parallel robots for special tasks that require accuracy, e.g. as assembly of electronic components.

Several robot architectures for high-speed operations have been proposed in the past decades [4–8]. Many of them have four degrees of freedom (DOF): three translations and one rotation about a fixed axis, i.e., a Schoenflies motion [9]. Some simple operations need only two translational DOF in order to move a part from a working area to another. Therefore, several robot architectures with two translational DOF have been proposed. Among them, those that have the capacity to fix the orientation of the platform via the use of a planar parallelogram (also called a Π joint) are necessary in numerous operations [8, 10–12]. However, most of the proposed architectures are not stiff enough along the normal to the plane of motion. As a consequence, the IRSBot-2 has been developed and outperforms its 2-DOF counterparts in terms of stiffness along the normal to the plane of motion [13].

This paper deals with the design optimization of the IRSBot-2 for fast and accurate pick-and-place operations such as the assembly of electronic components. The obtained optimal design will be used for the realization of an industrial prototype of

the IRSBot-2 in the scope of the French National Project ANR–2011–BS3–006–01–ARROW[1].

The pick-and-place operation is commonly used by industrial robots involved in both primary handling and case packing [13, 14]. The operation transfers an object from one position to another one in a workspace [13]. This standardized geometric path is referred to as the Adept cycle and its most used dimensions are $h = 25mm$ and $l = 300mm$ [3].

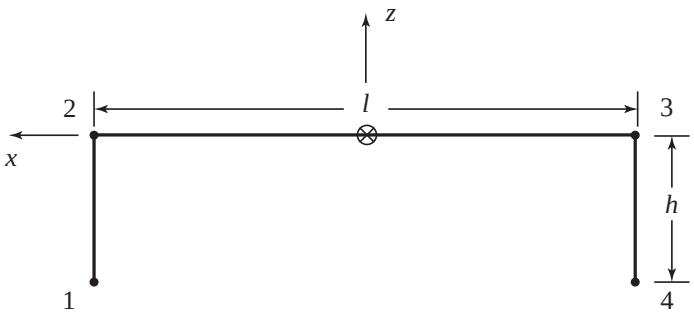

FIGURE 1. PICK-AND-PLACE TRAJECTORY.

The standard adept cycle, shown in Fig. 1, has square corners that introduce discontinuities in acceleration when traversed. To overcome these discontinuities, extremely high torques must be generated at the actuators, this, coupled with the inertial effect of the moving system, give rise to unwanted vibrations. To remove these discontinuities, the corners must be smoothed [14, 15]. However, the way to smooth the corner is not unique and, if the trajectory is not designed correctly, it can lead to very high vibrations of the end-effector [16] because the acceleration on the path is much too high.

In this paper, an optimization problem is first formulated to determine the optimal test trajectory that will be used in the design optimization process. This problem aims at finding the path defined with s-curves and the time trajectory that minimize the cycle time while the maximum acceleration of the moving platform remains lower than 20 G and the time trajectory functions are C_2 continuous.

Then, for simplifying the optimization procedure, two design optimization problems are formulated to find the optimal design parameters of the IRSBot-2 based on the previous optimal test trajectory. The first problem deals with the geometric and kinematic performances of the manipulator. The second problem considers elastostatic, dynamic and elastodynamic performances. Those two problems are expressed in such a way that they do not have any common decision variable and that the objective function and constraints of the first problem do not depend on the decision variables of the second problem. As a result, the two problems can be solved in cascade.

The first design optimization problem aims at finding the design parameters that minimize the size of the IRSBot-2 in the plane of motion for a prescribed regular dexterous workspace by considering only kinematic and kinetostatic constraints. The second design optimization problem allows the computation of the remaining design parameters that minimize the mass in motion and the size of the manipulator along the normal to the plane of motion and maximize the first natural frequency of the IRSBot-2 along the optimized test trajectory. This problem is subject to a set of constraints related to the elastostatic and dynamic performance of the robot.

Finally, the optimal design parameters are given and will be used for the development of an industrial prototype of the IRSBot-2.

2 ROBOT ARCHITECTURE

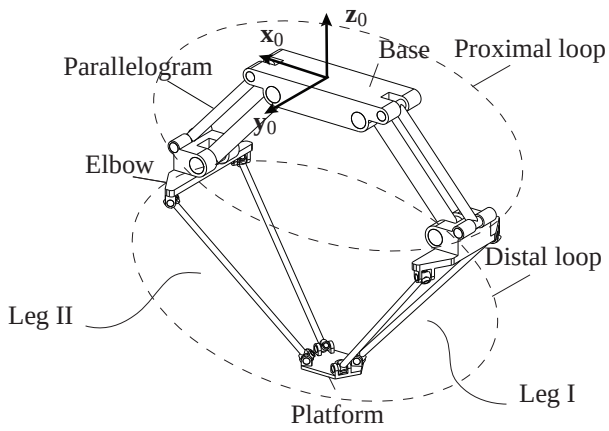

FIGURE 2. CAD MODELING OF THE IRSBOT-2.

The IRSBot-2 is shown in Fig. 2. It is a two degree-of-freedom translational parallel manipulator dedicated to fast and accurate pick-and-place operations. The IRSBot-2 is composed of two identical spatial limbs, each one containing a proximal module and a distal module.

The kth leg of the IRSBot-2 is described in Fig. 3 and contains one proximal module and one distal module ($k = I, II$). Therefore, the IRSBot-2 has one proximal loop and one distal loop shown in Fig. 2. The former is composed of the two proximal modules and the base. The latter is composed of the two distal modules and the moving-platform.

On the one hand, the proximal module amounts to a Π joint of normal $\mathbf{y}_0$ and is made up of links ℓ_{0k}, ℓ_{1k}, ℓ_{2k} and ℓ_{3k}. The

[1] http://arrow.irccyn.ec-nantes.fr/

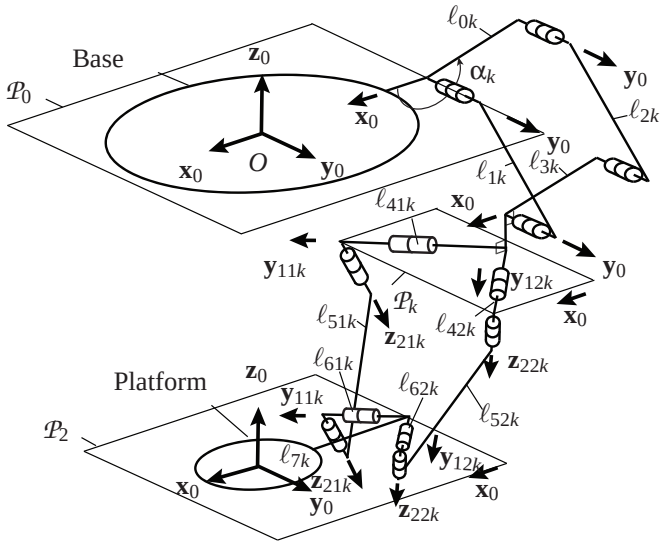

FIGURE 3. KINEMATIC CHAIN OF THE kTH LEG ($k = I, II$).

proximal module aims to keep planes $\mathcal{P}_0$ and $\mathcal{P}_k$ parallel. The base frame $(O, \mathbf{x}_0, \mathbf{y}_0, \mathbf{z}_0)$ is attached to plane $\mathcal{P}_0$.

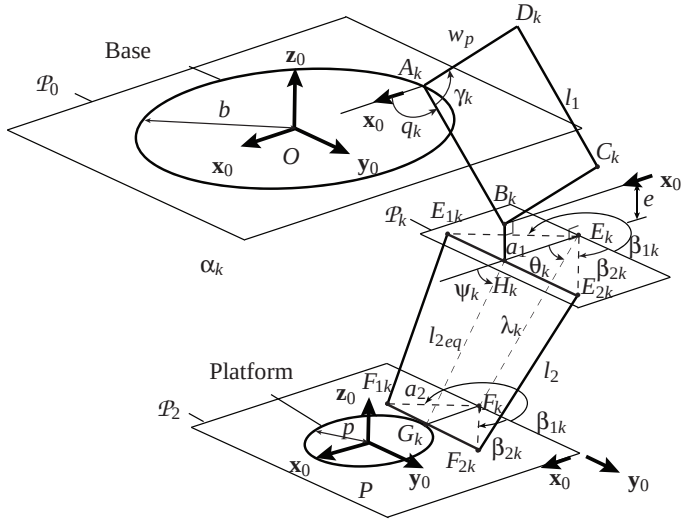

FIGURE 4. PARAMETERS OF THE kTH LEG ($k = I, II$).

On the other hand, the distal module is attached to link ℓ_{3k} of the parallelogram through two revolute joints of axis $(E_k, \mathbf{y}_{1jk})$ lying in plane $\mathcal{P}_k$ and to link ℓ_{7k} of the moving platform through two revolute joints of axis $(F_k, \mathbf{y}_{1jk})$ lying in plane $\mathcal{P}_2$ ($j = 1, 2$). Axes $\mathbf{y}_{11k}$ and $\mathbf{y}_{12k}$ ($\mathbf{z}_{21k}$ and $\mathbf{z}_{22k}$, resp.) are symmetrical with respect to plane $(\mathbf{x}_0 O \mathbf{z}_0)$. It should be mentioned that axes $\mathbf{y}_{1jk}$ and $\mathbf{z}_{2jk}$ are orthogonal and link ℓ_{5jk} lies in the plane normal to $\mathbf{z}_{2jk}$. Links ℓ_{51k} and ℓ_{52k} (links ℓ_{41k} and ℓ_{42k}, resp.) are not parallel, otherwise the distal module would become a spatial parallelogram and the robot architecture would be singular. The distal module may be decomposed into two identical parts composed of links ℓ_{4jk}, ℓ_{5jk} and ℓ_{6jk}, which are linked together with revolute joints of axes $\mathbf{z}_{2jk}$. The robot is assembled in such way that planes $\mathcal{P}_k$ and $\mathcal{P}_2$ remain parallel. Therefore, $\mathcal{P}_2$ is also parallel to $\mathcal{P}_0$.

The design parameters of the IRSBot-2 are depicted in Fig. 4 [13]. q_k is the actuated joint coordinate of the kth leg, $b = OA_k$ is the radius of the base, $l_1 = A_k B_k$ is the length of the proximal legs, $l_2 = E_{jk} F_{jk}$ is the length of the spatial distal legs and l_{2eq} is their projection length into the plane $(\mathbf{x}_0 O \mathbf{z}_0)$, w_{Pa} is the width of the parallelogram, a_1 and a_2 denote the lengths of segments $E_k E_{jk}$ and $F_k F_{jk}$, respectively. One can notice that the angle between $\mathbf{y}_0$ and $E_k E_{jk}$ (resp. $\mathbf{y}_0$ and $F_k F_{jk}$) is constant and equal to β_{jk}. Let β denote $\beta_{2II} = \beta$, then $\beta_{1I} = \pi + \beta$, $\beta_{2I} = -\beta$ and $\beta_{1II} = \pi - \beta$. Angle β is strictly bounded between 0 and $\pi/2$, i.e., $0 < \beta < \pi/2$, as links ℓ_{41k} and ℓ_{42k} can not be parallel. Finally, γ_k is the aperture angle of the parallelogram of the kth leg. α_k denotes the orientation angle of the fixed segment of the kth parallelogram as shown in Fig. 8.

prox$_1$ denotes the actuated proximal arms. *prox*$_2$ denotes the passive proximal arms. *elb* denotes the elbow that is composed of segments $C_k B_k$, $B_k H_k$ and $E_{2k} E_{1k}$. *dist* denotes the distal arms and EE denotes the moving-platform. Let M_ν and S_ν be the mass and the section of body ν, ν standing for *prox*$_1$, *prox*$_2$, *elb* or *dist*. The foregoing bodies have hollow cylindrical cross-sections of outer diameter $\phi_{o\nu}$ and thickness t_ν except for the moving-platform that can be seen as a parallelepiped of length, height and width equal to $2p$, h_{EE}, w_{EE}, respectively.

The parameters of the IRSBot-2 are classified with regard to their type below:

Lengths: l_1, l_2, b, p, w_{Pa}, e, a_1 and a_2;
Angles : β and α_k;
Cross-section parameters : $\phi_{o\nu}$, t_ν, h_{EE}, w_{EE}.
Material : E: Young Modulus; ρ: material density; G shear modulus.

After some discussions with industrial partners in the scope of the French National Project ANR–2011–BS3–006–01–ARROW, the specifications that the IRSBot-2 should satisfy are summed up in Tab. 1. The the robot should be as compact as possible due to some industrial constraints. Moreover, in order to minimize the robot vibrations due to the high accelerations, the natural frequencies should be as high as possible. Besides, a project partner imposes the use of TMB140–70 ETEL direct drive motors on us for the actuation of the IRSBot-2. Table 2 gives the characteristics of the TMB140–70 ETEL motor [2]:

[2] http://www.etel.ch/torque_motors/TMB

TABLE 1. SPECIFICATIONS FOR THE IRSBot-2

Accuracy ε_{lim}	20 μm
Acceleration max	20 G
Cycle time	200 ms
Path	25 mm $\times$ 300 mm $\times$ 25 mm
Regular workspace size	800 mm $\times$ 100 mm
Deformation $\boldsymbol{\delta}_{tlim}$ under a force $\mathbf{f}_s = [0, 20, 0]$ N and a moment $\mathbf{m}_s = [0.1, 0.1, 0.1]$ N.m	[0.5, 0.5, 0.5] mm, [0.5, 0.5, 0.5] deg
Payload	0.5 Kg

TABLE 2. DATASHEET OF THE TMB140–70 ETEL MOTOR

V_{max}	r	T_{peak}	T_C	Φ	J
[rpm]	[pt/rev]	[Nm]	[Nm]	[mm]	[Kg.m^{-2}]
600	200000	89.1	45	166	$2.3e^{-3}$

V_{max} is the maximal motor velocity; T_{peak} is the peak torque; T_C is the continuous torque; Φ is the motor external diameter; J is the rotor inertia; r is the encoder resolution.

Table 1 shows the global dimensions of the Adept cycle, the cycle time and the maximal end-effector acceleration. Nevertheless, the path and motion generator are not strictly defined. Consequently, a test trajectory is optimized in Sec. 3 in order to minimize the cycle time and to be sure that the acceleration of the moving-platform remains lower than 20 G. The corresponding optimal test trajectory will be also used later to verify that the required motor torques can be achieved by the TMB140–70 ETEL motors.

3 OPTIMAL TEST TRAJECTORY

S-curves are used to determine the optimal test trajectory for a matter of simplicity. The optimal test trajectory is expected to minimize the cycle time while the maximum acceleration of the moving-platform of the IRSBot-2 remains lower than 20 G along the path. An optimization problem is formulated and solved in this section in order to find the optimal test trajectory.

3.1 Trajectory Definition

As mentioned in Table 1, the IRSBot-2 must be capable of producing a test cycle in at most 200 ms. The path adopted for the manipulator design is illustrated in Fig. 5. This path is smoother than thus presented in Fig. 1 to avoid acceleration discontinuities and actuators deteriorations. It consists of:

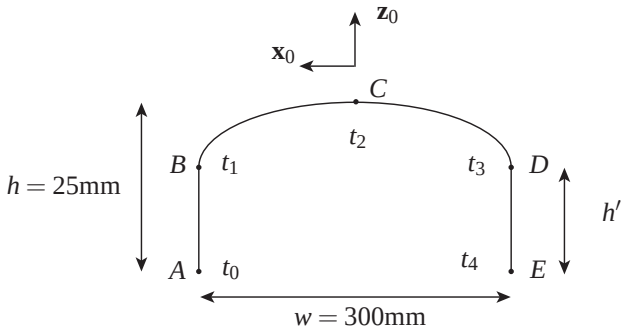

FIGURE 5. PATH ADOPTED FOR THE MANIPULATOR DESIGN.

(a) a vertical segment from point A to point B of length h';
(b) a curve BD, which is symmetrical with respect to the vertical line passing through point C and of direction $\mathbf{z}_0$. C is the mid-point of the path;
(c) a vertical segment from point D to point E of length h'.

The witdth w of the path is equal to 300 mm and its height h is equal to 25 mm. Let t_0, t_1, t_2, t_3 and t_4 be the trajectory time at points A, B, C, D and E, respectively. As A is the starting point of the trajectory, $t_0 = 0$ s and $t_2 = t_4/2$ and $t_3 = t_4 - t_1$ because of the symmetry of the trajectory.

z_A is the z–coordinate of point A expressed in the robot base frame $\mathcal{F}_b$ defined as $(O, \mathbf{x}_0, \mathbf{y}_0, \mathbf{z}_0)$.

The trajectory is defined in the $(\mathbf{x}_0 O \mathbf{z}_0)$ plane with parametric piecewise-polynomials as a function of time t, i.e., $x(t)$ and $z(t)$. Each polynomial-continuous function is of degree 5 for the acceleration profile to be continuous with respect to time. As a consequence, $z(t)$ is expressed with four piecewise-polynomial continuous functions:

$$z(t) = \begin{cases} z_1(t) = h' s_1(t) + z_A, & \text{if } t \in [t_0, t_1[\\ z_2(t) = (h - h') s_2(t) + h' + z_A, & \text{if } t \in [t_1, t_2[\\ z_3(t) = -(h - h') s_3(t) + h + z_A, & \text{if } t \in [t_2, t_3[\\ z_4(t) = -h' s_4(t) + h' + z_A, & \text{if } t \in [t_3, t_4] \end{cases} \quad (1)$$

Likewise, $x(t)$ is expressed with three piecewise-polynomial continuous functions to go from point A to point E, namely,

$$x(t) = \begin{cases} x_1(t) = w/2, & \text{if } t \in [t_0, t_1[\\ x_2(t) = -w s_5(t) + w/2, & \text{if } t \in [t_1, t_3[\\ x_3(t) = -w/2, & \text{if } t \in [t_3, t_4] \end{cases} \quad (2)$$

where $s_k(t)$ with $k = 1, \ldots, 5$ take the form:

$$s_k(t) = a_k t^5 + b_k t^4 + c_k t^3 + d_k t^2 + e_k t + f_k \quad (3)$$

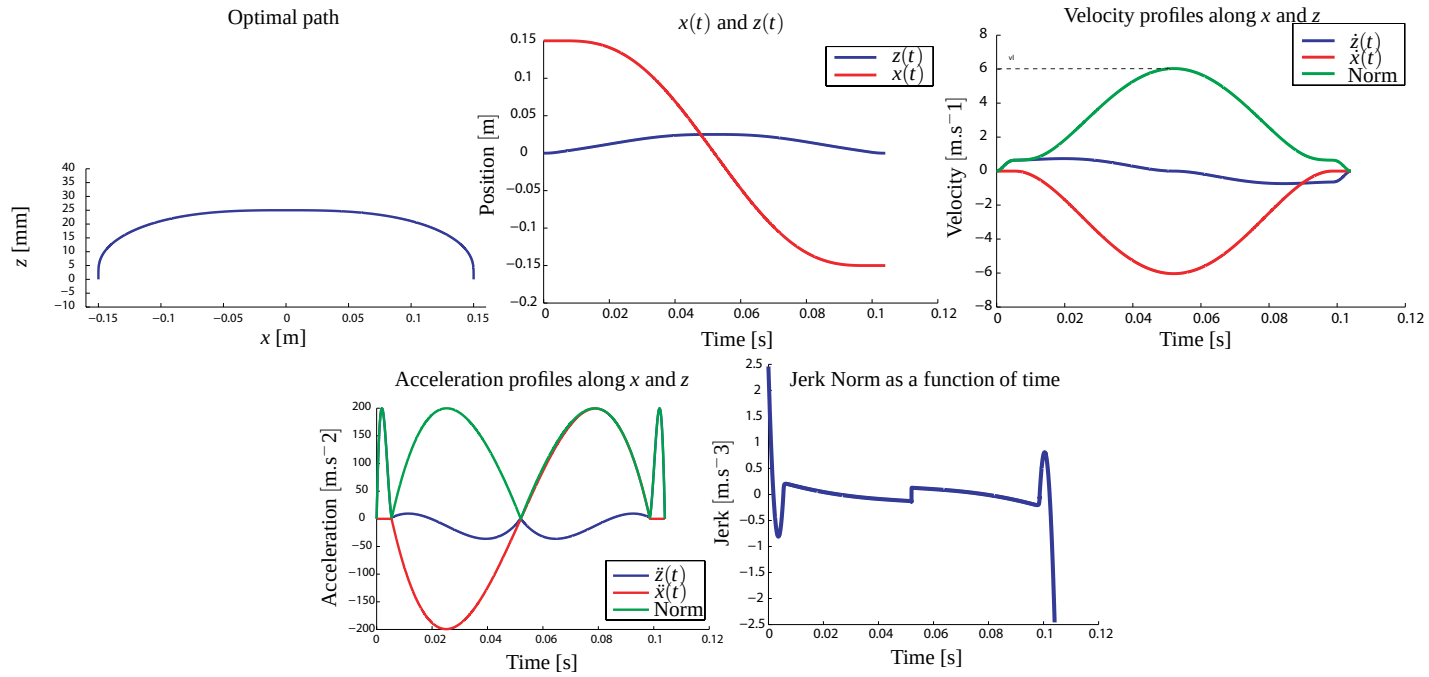

FIGURE 6. OPTIMAL PATH AND OPTIMAL VELOCITY, ACCELERATION AND JERK PROFILES.

The boundary conditions are defined as follows:

$$\begin{cases} s_1(t_0)=0\ \dot{s}_1(t_0)=0 & \ddot{s}_1(t_0)=0 \\ s_1(t_1)=1\ \dot{s}_1(t_1)=v_B/h' & \ddot{s}_1(t_1)=a_B/h' \\ \\ s_2(t_1)=0\ \dot{s}_2(t_1)=v_B/(h-h') & \ddot{s}_2(t_1)=a_B/(h-h') \\ s_2(t_2)=1\ \dot{s}_2(t_2)=0 & \ddot{s}_2(t_2)=0 \\ \\ s_3(t_2)=0\ \dot{s}_3(t_2)=0 & \ddot{s}_3(t_2)=0 \\ s_3(t_3)=1\ \dot{s}_3(t_3)=v_B/(h-h') & \ddot{s}_3(t_3)=-a_B/(h-h') \\ \\ s_4(t_3)=0\ \dot{s}_4(t_3)=v_B/h' & \ddot{s}_4(t_3)=-a_B/h' \\ s_4(t_4)=1\ \dot{s}_4(t_4)=0 & \ddot{s}_4(t_4)=0 \\ \\ s_5(t_1)=0\ \dot{s}_5(t_1)=0 & \ddot{s}_5(t_1)=0 \\ s_5(t_3)=1\ \dot{s}_5(t_3)=0 & \ddot{s}_5(t_3)=0 \end{cases} \tag{4}$$

where v_B and a_B are the velocity and acceleration of the moving-platform at point B, respectively. Note that $-v_B$ and a_B are the velocity and acceleration of the moving-platform at point D, respectively, due to the symmetry of the trajectory.

For given t_4, t_1, h', v_B, and a_B values, Eqs. (3) and (4) lead to a system of 30 linear equations with the 30 unknowns a_k, b_k, c_k, d_k, e_k, f_k, $k=1,\ldots,5$ that can be solved easily.

3.2 Optimization Problem Formulation

In order to find the trajectory that minimizes the cycle time t_4, whereas the maximum acceleration of the moving-platform of the IRSBot-2 remains lower than 20 G along the path, the following optimization problem should be solved:

$$\begin{aligned} \text{minimize} \quad & t_4 \\ \text{over} \quad & \mathbf{x} = \begin{bmatrix} t_4\ t_1\ h'\ v_B\ a_B \end{bmatrix} \\ \text{subject to} \quad & \max\sqrt{\ddot{x}^2(t)+\ddot{z}^2(t)} \leq 20\ G \quad \forall t \in [t_0, t_4] \\ & t_1 < t_4/2 \\ & 2\ \text{mm} \leq h' \leq h \end{aligned} \tag{5}$$

The decision variables t_4, t_1, h', v_B, a_B of this optimization problem are the components of decision variable vector $\mathbf{x}$.

Optimization problem (5) was solved by means of MATLAB *fmincon* function using multi-starting points. The optimum decision variables of problem (5) are gathered in Table 3 and characterize the optimal test trajectory.

Figure 6 illustrates the obtained optimal test trajectory, namely, the optimal path adopted for the IRSBot-2 design and the optimal velocity, acceleration and jerk profiles.

TABLE 3. OPTIMUM DECISION VARIABLES OF PB (5).

t_4 [s]	t_1 [s]	h' [mm]	v_B [m.s^{-1}]	a_B [m.s^{-2}]
0.1041	0.0055	2	0.6205	4.5313

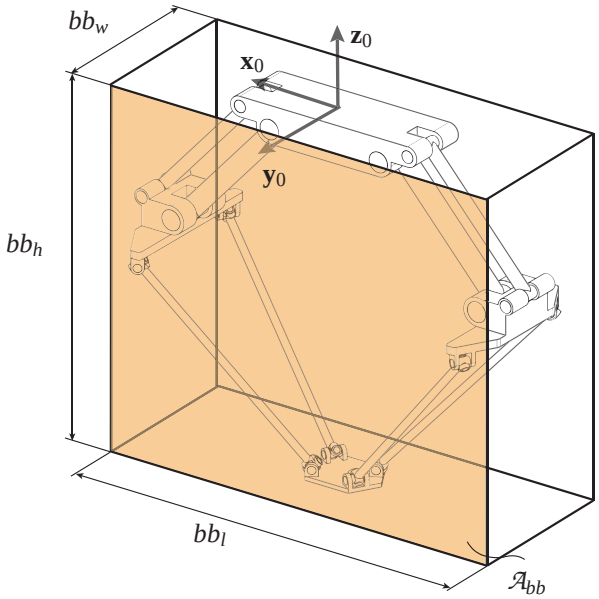

FIGURE 7. BOUNDING BOX OF THE IRSBOT-2.

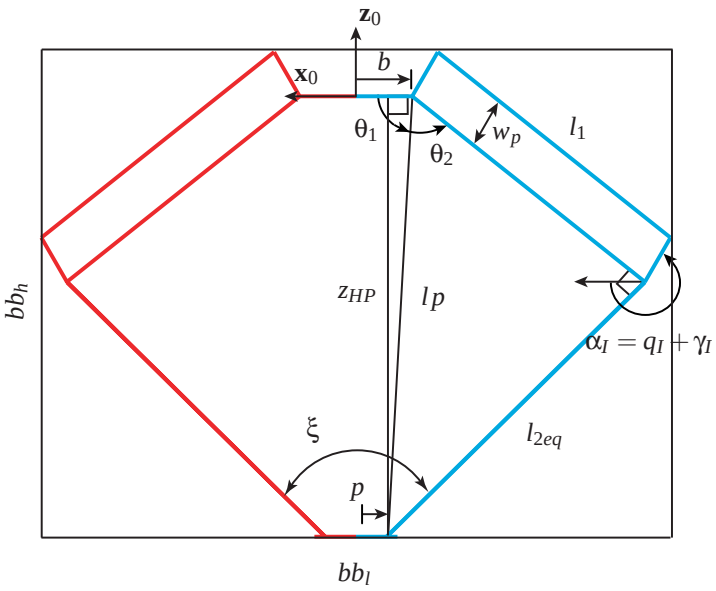

FIGURE 8. HOME CONFIGURATION OF THE IRSBOT-2.

4 FIRST DESIGN OPTIMIZATION PROBLEM

The first design optimization problem aims at finding the design parameters that minimize the size of the IRSBot-2 in the plane of motion for a prescribed regular dexterous workspace, taking into account only kinematic and kinetostatic constraints. The problem formulation is described thereafter.

4.1 Objective Function

The objective function of the optimization problem corresponds to the size of the projection of the IRSBot-2 into the plane of motion $(\mathbf{x}_0 O \mathbf{z}_0)$ as the manipulator should be as compact as possible.

The objective function amounts to the surface area $\mathcal{A}_{bb}$ of the bounding parallelepiped rectangle shown in Fig. 7. The surface area $\mathcal{A}_{bb}$ is calculated for the IRSBot-2 in its home configuration, which is depicted in Fig. 8. Leg I and leg II are symmetrical with respect to plane $(\mathbf{y}_0 O \mathbf{z}_0)$ and the distal and proximal modules are perpendicular to each other in this configuration. Therefore, $\mathcal{A}_{bb}$ is expressed as follows,

$$\mathcal{A}_{bb} = bb_l \, bb_h \tag{6}$$

bb_l and bb_h are the length and the height of the bounding parallelepiped rectangle and take the form:

$$bb_l = 2(b - w_p \cos(\alpha_I) - l_1 \cos(q_1)) \tag{7a}$$
$$bb_h = -z_{HP} - w_p \sin(\alpha_I) \tag{7b}$$

with

$$z_{HP} = -\sqrt{l_1^2 + l_{2eq}^2 - (b-p)^2} \tag{8a}$$
$$q_1 = \theta_1 + \theta_2 \tag{8b}$$
$$\theta_1 = \arccos((b-p)/lp) \tag{8c}$$
$$\theta_2 = \arccos(l_1/lp) \tag{8d}$$
$$l_p = \sqrt{l_1^2 + l_{2eq}^2} \tag{8e}$$

4.2 Decision Variables

The decision variables of the first design optimization problem are the design parameters of the IRSBot-2 that affect $\mathcal{A}_{bb}$ as well as the workspace size and the kinematic performances of the manipulator, namely,

$$\mathbf{x}_1 = \left[l_1 \; l_{2eq} \; b \; p \; \alpha_I \right] \tag{9}$$

l_1, l_{2eq}, b, p and α_I are depicted in Fig. 4 and defined in Sec. 2.

The offset e, shown in Fig. 4, may also affect $\mathcal{A}_{bb}$, but is supposed to be null for a matter of clarity.

4.3 Optimization Problem Formulation

From Tab. 1, the IRSBot-2 should cover a rectangular shaped workspace, called Regular Workspace RW, of length $w_l = 800$ mm and height $w_h = 100$ mm. Some geometric and

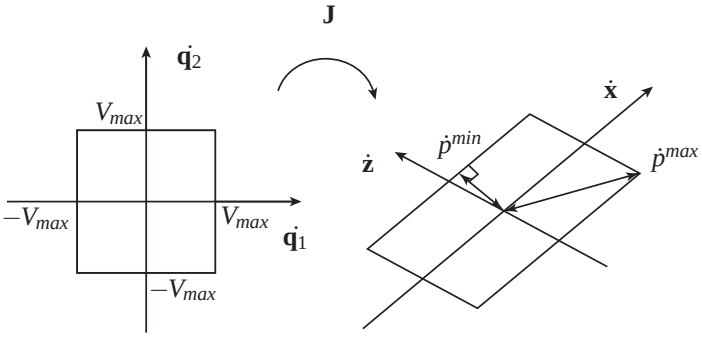

FIGURE 9. TRANSMISSION FACTOR.

kinematic constraints should be also satisfied throughout *RW*, thus obtaining a Regular Dexterous Workspace (*RDW*), for the IRSBot-2 to respect the specifications described in Tab. 1. Let *LRDW* denote the Largest Regular Dexterous Workspace of the manipulator.

The design problem aims at finding the decision variable vector $\mathbf{x}_1$ that minimizes the surface area $\mathcal{A}_{bb}$ while the length l_{LRDW} and the height h_{LRDW} of *LRDW* are higher or equal than w_l and w_h, respectively. The base radius b of the manipulator should be also larger than the motor external radius $\Phi/2$ defined in Tab. 2. The base radius b should be larger than the moving-platform radius p too. Thus, the design optimization problem is formulated as follows,

$$\begin{aligned} \text{minimize} \quad & \mathcal{A}_{bb} \\ \text{over} \quad & \mathbf{x}_1 = \begin{bmatrix} l_1 & l_{2eq} & b & p & \alpha_I \end{bmatrix}^T \\ \text{subject to} \quad & l_{LRDW} \geq w_l \\ & h_{LRDW} \geq w_h \\ & b \geq p \\ & b > \Phi/2 \end{aligned} \tag{10}$$

The methodology used to determine *LRDW* for a given decision variable vector $\mathbf{x}_1$ is explained thereafter.

4.4 Largest Regular Dexterous Workspace

The following geometric and kinematic constraints should be respected throughout a Regular Workspace *RW* for the latter to become Regular Dexterous Workspace *RDW*:

1. The assembly of the manipulator should be possible.
2. The IRSBot-2 should not reach any parallel singularity throughout *RW* [17];
3. In order to avoid the degeneracy of the parallelogram joints, the following constraints are fixed:

$$\pi/6 \leq \gamma_I \leq 5\pi/6 \tag{11a}$$
$$\pi + \pi/6 \leq \gamma_{II} \leq \pi + 5\pi/6 \tag{11b}$$

   γ_k being equal to $\alpha_k - q_k$, $k = I, II$.
4. Velocity transmission: From Fig. 6, the IRSBot-2 should be able to reach a velocity equal to $v^{lim} = 6$ m.s^{-1} throughout *RW*. Knowing the maximum motor velocity V_{max} from Tab. 2 and the kinematic Jacobian matrix $\mathbf{J}$ of the manipulator from [13], Fig. 9 can be used to find the minimum velocity transmission $\dot{p}^{min}$ at any point of *RW* [18]. Therefore, the following constraint should be satisfied throughout *RW*:

$$\dot{p}^{min} > v^{lim} \tag{12}$$

5. Error transmission: Knowing the resolution r of the motor encoders from Tab. 2, the maximum point-displacement δp^{max} of the moving-platform due to encoder errors can be assessed with matrix $\mathbf{J}$. Therefore, δp^{max} should be lower than ε_{lim} throughout *RW*, ε_{lim} being given in Tab. 1.
6. The forces exerted into the passive joints are proportional to $1/\sin\xi$ [19], ξ being the angle between the distal modules and shown in Fig. 8. Consequently, it is decided that $\sin\xi$ should be higher than 0.1 throughout *RW* to avoid excessive effort in the joints.

Algorithm 1 is used to find the LRDW amongst the RDWs of the manipulator [18] for a given decision variable vector $\mathbf{x}_1$.

$\{G_{ij}\}$ defines the workspace grid that includes the manipulator workspace $RDW = w_l \times w_h$ and possesses uniform but different steps along the Cartesian axes, namely ($L_G = d_x N_0 \times H_G = d_z N_0$), where L_G and H_G define the length and the height of the workspace grid, d_x and d_z the discretisation pitch along $\mathbf{x}_0$ and $\mathbf{z}_0$, and N_0 the number of nodes in each direction. Besides, let us define a 2D binary matrix $\Omega_{ij} \in \{0, 1\}$, where $\Omega_{ij} = 1$ if the foregoing geometric and kinematic constraints are all satisfied at node G_{ij}, $\Omega_{ij} = 0$ otherwise. For computation convenience, $\Omega_{ij} = 0$ if $\{G_{ij}\}$ does not belong to *RDW*.

Then we look for the largest sub-matrix inside $\{\Omega_{ij}\}$ containing non-zero values only. Algorithm 1 uses an additional integer matrix $\{\Phi_{ij}\}$ that defines the size of the candidate solutions workspace with the vertex G_{ij}.

4.5 Optimal Solution of Problem (10)

A genetic algorithm, i.e., the MATLAB *ga* function, was used to solve problem (10). It converged after six generations with a population containing 150 individuals. Then, a local optimum $\mathbf{x}_1^*$ was obtained with the MATLAB *fmincon* function, taking the best individual of the final population as the starting point.

Algorithm 1: DETERMINATION OF THE LARGEST REGULAR DEXTEROUS WORKSPACE.

Input: $\{\Omega_{ij}\}, \{G_{ij}\}, d_x, dz$
Output: $l_{LRDW}, h_{LRDW}, (i_0, j_0)$

$\Phi_{ij} = 0$;
for $\{i = 1 \& \forall j\} \cup \{j = 1 \& \forall i\}$ **do**
  $\Phi_{ij} = \Omega_{ij}$
end
;
for $i = 2 : N_0$ **do**
  for $j = 2 : N_0$ **do**
    if $\Omega_{ij} = 1$ **then**
      $\Phi_{ij} = 1 + min\{\Phi_{i-1,j}, \Phi_{i,j-1}, \Phi_{i-1,j-1}\}$
    end
  end
end
;
Find $d = max(\Phi_{ij}) - 1; (i_0, j_0) = argmax(\Phi_{ij})$;
Retrieve from the grid $\{G_{ij}\}$ the desired square bounded by the indices $(i_0 - d, j_0 - d)$ and (i_0, j_0);
Give $l_{LRDW} = d_x d$ and $h_{LRDW} = d_z d$;

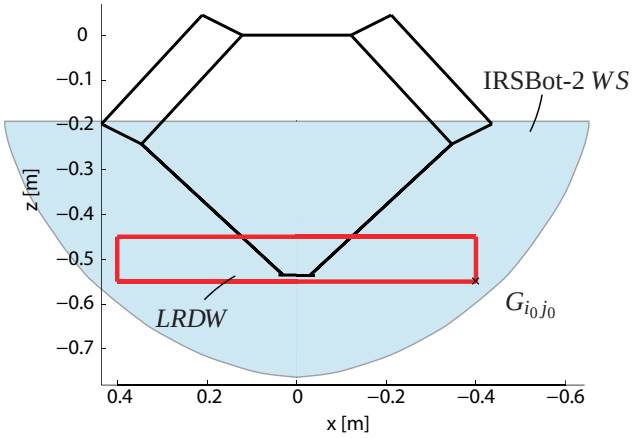

FIGURE 10. OPTIMAL 2D-DESIGN OF THE IRSBOT-2 AND LARGEST REGULAR DEXTEROUS WORKSPACE (SCALED)

The optimal design variables of problem (10) and the associated surface area $\mathcal{A}_{bb}$ are given in Tab.4. The corresponding dimensions of the IRSBot-2 and LRDW are depicted in Fig. 10.

5 SECOND DESIGN OPTIMIZATION PROBLEM

The second design optimization problem aims to find the design parameters that minimize the mass in motion and the size of the manipulator along the normal to the plane of motion and maximize the first natural frequency of the IRSBot-2 at both ends of the optimized test trajectory. This problem is also subject to a set of constraints related to the elastostatic and dynamic performance of the robot. The required actuated torques should be also smaller than the maximum torque provided by the motors along the trajectory.

TABLE 4. OPTIMAL SOLUTION OF PROBLEM (10)

$\mathcal{A}_{bb}$ [m^2]	l_1 [mm]	l_{2eq} [mm]	b [mm]	p [mm]	α_I [rad]
0.2528	331.08	430.56	121.42	30.20	-2.6774

A simplified planar dynamic model of the manipulator and an elastic model are taken from [16] and [13], respectively. An elastodynamic model has been written to compute the natural frequencies of the robot. This model is not described in this paper, but is based on the methodology presented in [20]. The elastodynamic model could be used instead of the elastostatic model to evaluate the robot deformations under external loading. However, the former is more time consuming than the latter.

The links of the IRSBot-2 are made up of Duraluminum. Its Young modulus $E = 74$ MPa, its shear modulus $G = 27.8$ MPa and its density $\rho = 2800$ Kg.m^{-3}. The links have hollow cylindrical cross-sections and are supposed to have the same thickness th in order to minimize the number of decision variables.

5.1 Three Objective Functions

The optimization problem is multi-objective and contains three objective functions. The first objective function is the width bb_w of the bounding box shown in Fig. 7 and is defined as follows:

$$bb_w = 2\,a_1 \cos\beta \tag{13}$$

The second objective function is the mass M_{IRS} in motion of the manipulator and is expressed as:

$$M_{IRS} = 2M_{prox_1} + 2M_{prox_2} + 2M_{elb} + 4M_{dist} \tag{14}$$

with

$$M_{prox_1} = \rho\, l_1\, S_{prox_1} \tag{15a}$$
$$M_{prox_2} = \rho\, l_1\, S_{prox_2} \tag{15b}$$
$$l_{elb} = w_p + 2\,a_1 \cos(\beta) + e \tag{15c}$$
$$M_{elb} = \rho\, l_{elb}\, S_{elb} \tag{15d}$$
$$l_2 = \sqrt{l_{2eq}^2 + (a_1 - a_2)^2 (\cos(\beta))^2} \tag{15e}$$
$$M_{dist} = \rho\, l_2\, S_{dist} \tag{15f}$$

The natural frequencies of the manipulator are derived from its elastodynamic model obtained with the Matrix Structural Analysis method. Let $\mathbf{M}$ and $\mathbf{K}$ be the mass and stiffness matrices of the IRSBot-2, respectively. The natural frequencies of the manipulator are proportional to the square root of the eigenvalues of matrix $\mathbf{M}^{-1}\mathbf{K}$. Let f^1_{IRS} be the smallest frequency from the natural frequencies computed at both ends of the optimal trajectory. f^1_{IRS} is the third objective function of the optimization problem at hand.

Let bb_w^{max}, M_{IRS}^{max} and f_{IRS}^{1min} be the maximum value of bb_w, the maximum value of M_{IRS} and the minimum value of f^1_{IRS}, respectively. Those values were assessed by selecting 10000 designs randomly in the definition domain.

As a consequence, the three objective functions are normalized and weighted in order to convert the multi-objective optimization problem into mono-objective optimization problem. The obtained objective function f_{pb2} is expressed as:

$$f_{pb2} = 0.2\,\frac{bb_w}{bb_w^{max}} + 0.3\,\frac{M_{IRS}}{M_{IRS}^{max}} + 0.5\,\frac{f_{IRS}^{1min}}{f^1_{IRS}} \tag{16}$$

Note that f_{pb2} is bounded between 0 and 1. The weighting factors were chosen based on some discussions between the partners of the French National Project ANR–2011–BS3–006–01–ARROW.

5.2 Decision Variables

The decision variables of the optimization problem are the components of vector $\mathbf{x}_2$, namely,

$$\mathbf{x}_2 = \left[\, a_1 \;\; a_2 \;\; w_{Pa} \;\; \beta \;\; \phi_{oprox_1} \;\; \phi_{oprox_2} \;\; \phi_{odist} \;\; \phi_{oelb} \;\; th \,\right] \tag{17}$$

It is apparent that those decision variables, described in Sec. 2, do not affect the objective function and constraints of the first design optimization problem (10). Besides, the two design optimization problems do not have any decision variable in common. Consequently, they can be solved in cascade.

5.3 Constraints

The optimization problem is subject to a set of constraints related to the elastostatic and dynamic performance of the robot. First, the required motor torques should be lower than the peak torque T_{peak} given in Tab.2, $T_{Peak} = 89.1$ Nm, along the trajectory not to damage the motors. Then, the root-mean-square τ_{RMS} of the motor torques should be smaller than the continuous torque $T_C = 45$ Nm to avoid temperature increase.

Moreover, for a 20 N force exerted on the moving-platform along $\mathbf{y}_0$, the point-displacement of the latter should be smaller than 0.5 mm. Likewise, for a 0.1 Nm moment applied on the moving-platform about any axis, the corresponding orientation displacement of the moving-platform should be smaller than 0.5 deg. The foregoing constraints related to the manipulator stiffness are expressed as $\boldsymbol{\delta}_t^{max} \leq \boldsymbol{\delta}_{tlim}$ in the problem formulation.

5.4 Optimization Problem Formulation

The second design optimization problem can be formulated as follows,

$$\begin{aligned}
\text{minimize} \quad & f_{pb2} \\
\text{over} \quad & \mathbf{x}_2 = \left[\, a_1 \;\; a_2 \;\; w_{Pa} \;\; \beta \;\; \phi_{oprox_1} \;\; \phi_{oprox_2} \;\; \phi_{odist} \;\; \phi_{oelb} \;\; th \,\right] \\
\text{subject to} \quad & \tau_{max} \leq T_{Peak} \\
& \tau_{RMS} \leq T_C \\
& \boldsymbol{\delta}_t^{max} \leq \boldsymbol{\delta}_{tlim}
\end{aligned} \tag{18}$$

5.5 Optimal Solution of Problem (18)

A genetic algorithm was used to solve problem (18) and converged after seven generations, each population containing 50 individuals. Then, a local optimum decision variable vector $\mathbf{x}_2^*$ of optimization problem (18) was obtained with MATLAB *fmincon* function and is summed up in Tab. 5. The corresponding objective functions and constraint values are given in Tab. 6. The size of the robot and its shape are illustrated in Fig. 11.

6 CONCLUSION

This paper dealt with the design optimization of the IRSBot-2 based on an optimized test trajectory for fast pick and place operations. The goal was to minimize the size of the manipulator and its mass while maximizing its first natural frequency, as function of prescribed geometric, elastostatic and dynamic performances. This is a classical but rather complex problem because of the number of decision variables, constraints and criteria involved. To make the problem more tractable, it was decomposed into two independent problems that could be solved in cascade. The optimal test trajectory was defined in such a way that the cycle time is a minimum while the maximum acceleration of the moving platform remains lower than 20 G and the time trajectory functions are C_2 continuous. S-curves were used to define the path and the motion profile of the test trajectory simultaneously.

The optimal design of the IRSBot-2 minimizes the volume of its bounding box, its mass in motion and maximizes its first natural frequencies at both ends of the optimal test trajectory. This optimal design will be used for the realization of an industrial prototype of the IRSBot-2 later on. The design methodology followed for the IRSBot-2 will be further studied for application to other parallel manipulators.

TABLE 5. DESIGN PARAMETERS OF THE OPTIMAL DESIGN OF THE IRSBOT-2

a_1	a_2	w_{Pa}	β	ϕ_{oprox_1}	ϕ_{oprox_2}	ϕ_{odist}	ϕ_{oelb}	th
[mm]	[mm]	[mm]	[rad]	[mm]	[mm]	[mm]	[mm]	[mm]
183.131	36.345	80.675	0.76814	99.803	10	37.854	75.454	2

TABLE 6. OBJECTIVE FUNCTIONS AND CONSTRAINTS ASSOCIATED WITH THE OPTIMAL SOLUTION OF PROBLEM (18)

bb_w	M_{IRS}	f^1_{IRS}	τ_{max}	τ_{RMS}	δ_{tx}	δ_{ty}	δ_{tz}	δ_{rx}	δ_{ry}	δ_{rz}
[m]	[Kg]	[Hz]	[Nm]	[Nm]	[mm]	[mm]	[mm]	[deg]	[deg]	[deg]
0.26	2.15	52.31	75.88	44.03	0.001	0.104	0.001	0.033	0.003	0.006

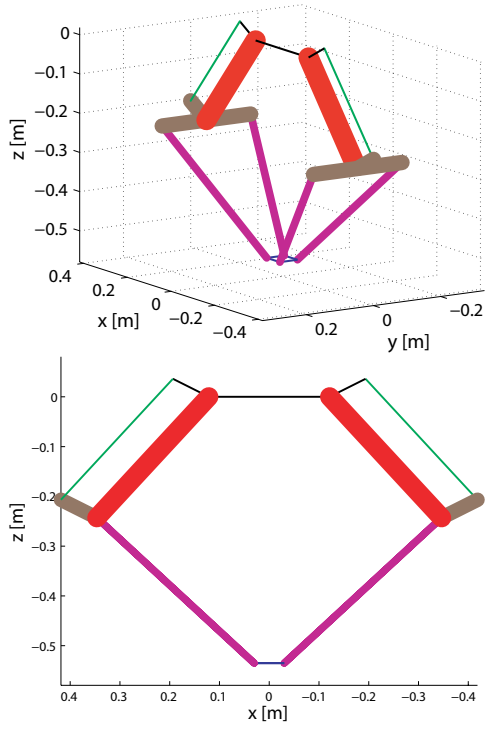

FIGURE 11. OPTIMAL DESIGN OF THE IRSBOT-2 (SCALED).

7 ACKNOWLEDGMENT

This work was conducted with the support of the French National Research Agency (Project ANR-2011-BS3-006-01-ARROW).

REFERENCES

[1] Clavel, R., 1990. Device for the movement and positioning of an element in space, December.

[2] Bonev, I. Delta parallel robot - the story of success. www.parallemic.org/Reviews/Review002.html. Article accessed November 2011.

[3] Inc., A. T. www.adept.com. Webpage accessed February 2011.

[4] Clavel, R., 1990. Device for the movement and positioning of an element in space. Patent US 4976582, December 11.

[5] Angeles, J., Caro, S., Khan, W., and Morozov, A., 2006. "Kinetostatic design of an innovative schonflies-motion generator". *Proceedings of IMechE Part C: Journal of Mechanical Engineering Science*, ***220***(7), Jan., pp. 935–943.

[6] Krut, S., Nabat, V., Company, O., and Pierrot, F., 2004. "A high-speed parallel robot for scara motions". In Robotics and Automation, 2004. Proceedings. ICRA '04. 2004 IEEE International Conference on, Vol. 4, pp. 4109 – 4115.

[7] Nabat, V., Pierrot, F., de la O Rodriguez Mijangos, M., Azcoita Arteche, J. M., Bueno Zabalo, R., Company, O., and Florentino Perez De Armentia, K., 2007. High-speed parallel robot with four degrees of freedom. Patent EP 1 870 214 A1.

[8] Liu, X., and Kim, J., 2002. "Two novel parallel mechanisms with less than six degrees of freedom and the applications". In Proc. Workshop on Fundamental Issues and Future Reserch Directions for Parallel Mechanisms and Manipulators, pp. 172–177.

[9] Caro, S., Khan, W. A., Pasini, D., and Angeles, J., 2010. "The rule-based conceptual design of the architecture of serial schönflies-motion generators". *Mechanism and Machine Theory*, ***45***(2), Feb., pp. 251–260.

[10] Brogardh, T., 2001. Device for relative movement of two elements. Patent US 6301988 B1.

[11] Huang, T., Li, M., Li, Z., Chetwynd, D., and Whitehouse, D., 2003. Planar parallel robot mechanism with two translational degrees of freedom. Patent WO 03055653 A1.

[12] Pierrot, F., Krut, S., Company, O., Nabat, V., Baradat, C., and Fernandez, A. S., 2009. Two degree-of-freedom parallel manipulator. Patent WO 2009/089916 A1.

[13] Germain, C., Briot, S., Glazunov, V., Caro, S., and Wenger, P., 2011. "Irsbot-2: A novel two-dof parallel robot for high-speed operations". In Proceedings of the ASME 2011 International Design Engineering Technical Conferences and

Computers and Information in Engineering Conference, Washington DC, USA.

[14] Gauthier, J.-F., Angeles, J., and Nokleby, S., 2008. "Optimization of a test trajectory for scara systems". *Advances in Robot Kinematics: Analysis and Design*, pp. 225–234.

[15] Kanayama, Y., and Miyake, N., 1985. "Trajectory generation for mobile robots". In International Symposium on Robotics Research, pp. 333 – 340.

[16] Barnard, C., Briot, S., and Caro, S., 2012. "Trajectory generation for high speed pick and place robots". In Proceedings of the ASME 2012 11th Biennial Conference On Engineering Systems Design And Analysis ESDA 2012, no. ESDA2012-82197.

[17] Germain, C., Caro, S., Briot, S., and Wenger, P., 2013. "Singularity-free design of the translational parallel manipulator irsbot-2". *Mechanism and Machine Theory,* ***64***(0), pp. 262 – 285.

[18] Briot, S., Pashkevich, A., and Chablat, D., 2010. "Optimal technology-oriented design of parallel robots for high-speed machining applications". In Robotics and Automation (ICRA), 2010 IEEE International Conference on, pp. 1155 –1161.

[19] Briot, S., Glazunov, V., and V., A., 2013. "Investigation on the effort transmission in planar parallel manipulators". *ASME Journal of Mechanisms ans Robotics*. in press.

[20] Briot, S., and Khalil, W., 2013. "Recursive symbolic calculation of the dynamic model of flexible parallel robots". In Proceedings of the 2013 IEEE International Conference on Robotics and Automation (ICRA 2013).